IEEE Photonics Journal
An IEEE Photonics Society Publication

Open Access

A Variable Step-Size Unconstrained Adaptive FD-LMS Algorithm for MDM Transmission

Volume 10, Number 2, April 2018

Guijun Hu
Chengbin Huang

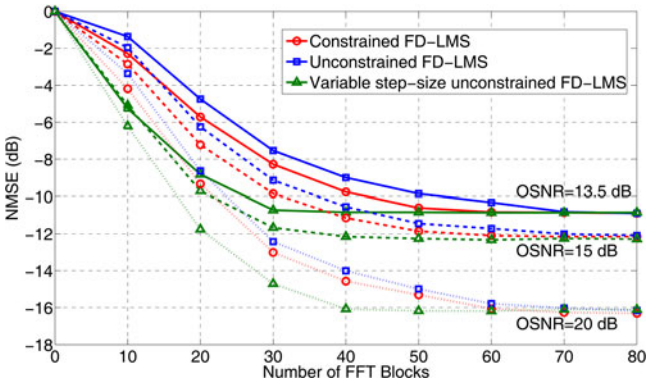

DOI: 10.1109/JPHOT.2018.2809004
1943-0655 © 2018 IEEE

IEEE photonics SOCIETY

IEEE

A Variable Step-Size Unconstrained Adaptive FD-LMS Algorithm for MDM Transmission

Guijun Hu and Chengbin Huang

College of Communication Engineering, Jilin University, Changchun 130012, China

DOI:10.1109/JPHOT.2018.2809004
1943-0655 © 2018 IEEE. Translations and content mining are permitted for academic research only. Personal use is also permitted, but republication/redistribution requires IEEE permission. See http://www.ieee.org/publications_standards/publications/rights/index.html for more information.

Manuscript received December 25, 2017; revised February 11, 2018; accepted February 20, 2018. Date of publication February 23, 2018; date of current version April 6, 2018. This work was supported in part by the National Natural Science Foundation of China under Grant 61575078, in part by Jilin Provincial Science and Technology Department under Grant 20140203009GX, and in part by Jilin Province Development and Reform Commission under Grant 2014Y087. Corresponding author: G. Hu (e-mail: hugj@jlu.edu.cn).

Abstract: Mode-division multiplexing (MDM) over few-mode fibers has been proposed to break through the Shannon limit of the single-mode fiber. Mode coupling and differential mode group delay are two major drawbacks, which limit the performance of the system. In this paper, a variable step-size unconstrained adaptive frequency-domain least mean square (FD-LMS) algorithm is proposed for demultiplexing in a 6×6 MDM transmission. In an 80 km link, at the 7% FEC threshold, the least required optical signal noise ratio (OSNR) for the proposed algorithm is about 13.5 dB, which is the same as the constrained FD-LMS algorithm and the unconstrained FD-LMS algorithm. Besides, the proposed algorithm can improve the convergence speed by 45.1% and 56.9% in comparison with the constrained FD-LMS algorithm and the unconstrained FD-LMS algorithm. For the distance of 2000 km, the computational complexity of the proposed algorithm is 52.8% lower than that of the constrained FD-LMS algorithm. The effect of mode-dependent loss (MDL) on the proposed algorithm is also explored. The result shows that the MDL tolerance of the proposed algorithm is similar to the constrained FD-LMS algorithm, and the OSNR penalty of the proposed algorithm is 0.5 dB higher than that of the constrained FD-LMS algorithm at a transmission distance of 800 km.

Index Terms: Demultiplexing, optical fiber communication, MIMO.

1. Introduction

In order to break through the Shannon limit of the single-mode fiber, mode-division multiplexing (MDM) using few-mode fibers (FMFs) has recently been proposed [1]–[4]. In an ideal MDM system, the total capacity of the system scales linearly with the number of modes. However, several factors will deteriorate the performance of the MDM system, such as mode coupling and differential mode group delay (DMGD) [5]–[7].

At the coherent receiver, multi-input multi-output (MIMO) equalization is an effective way to compensate these impairments [8], [9]. So far, several algorithms have been employed in the MIMO equalization [10]–[17]. Among them, the adaptive least mean square (LMS) algorithm attracts much attention as a result of robustness and simplicity. The LMS algorithm can be achieved in time-domain (TD) and frequency-domain (FD). In comparison to TD-LMS algorithm, FD-LMS algorithm reduces much complexity by fast Fourier transform (FFT). Based on the existence of the TD

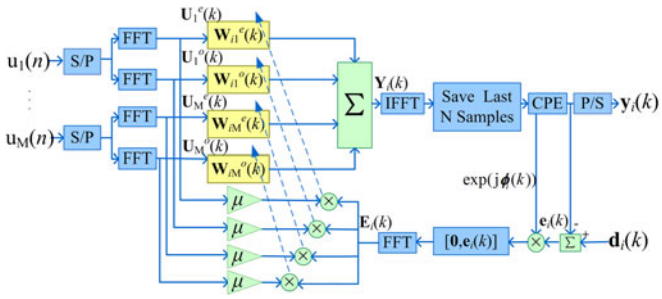

Fig. 1. The diagram of the unconstrained FD-LMS for each output in MDM transmission.

constraint in the adaptive process, FD-LMS algorithm can be classified into the constrained FD-LMS algorithm and the unconstrained FD-LMS algorithm. The unconstrained FD-LMS algorithm omits the additional FFT blocks (the TD constraint in the constrained algorithm), thus decreasing complexity [18]–[20]. The paper [21] has proven that the unconstrained FD-LMS algorithm is a good choice for coherent optical transmission in polarization-mode dispersion compensation. Recently, it has been demonstrated that the unconstrained FD-LMS algorithm has its effectiveness in MDM system [22].

In addition, the convergence speed of equalization algorithms is another key point to be considered [11]. Since it determines the length of training sequences used for the equalization algorithms, thus determining the spectral efficiency of the overall system. In LMS algorithm, the step-size determines the convergence speed. Higher step-size corresponds to higher convergence speed, but it will induce higher mean square error (MSE) [24]. Furthermore, the paper [23] points that the unconstrained FD-LMS algorithm needs lower step-size to attain the same MSE compared to the constrained FD-LMS algorithm, which in return further influences the convergence speed. The method of variable step-size has been proved to be an effective way to meet the requirements of fast convergence speed and small misadjustment [24]. However, to the best of our knowledge, no one has made the variable step-size analysis for the unconstrained FD-LMS algorithm in an MDM system until now.

In this paper, a variable step-size unconstraint adaptive FD-LMS algorithm is proposed to compensate DMGD in MDM transmission system, which utilizes the bin-wise block-varying step-size method in [25] to optimize the step-size. In a 6 $\times$ 6 MDM simulation system, we compare the proposed algorithm with the unconstrained FD-LMS algorithm and the conventional constrained FD-LMS algorithm in equalization performance, convergence speed and complexity. The proposed algorithm shows similar equalization performance with the constrained FD-LMS algorithm and the unconstrained FD-LMS algorithm. In an 80 km transmission system at 13.5 dB optical signal noise ratio (OSNR), it improves the convergence speed by 45.1% and 56.9% than the constrained FD-LMS algorithm and the unconstrained FD-LMS algorithm, respectively. For a transmission distance of 2000 km, it can reduce the complexity by 52.8% compared with the constrained FD-LMS algorithm. In the end, the influence of mode-dependent loss (MDL) on our proposed algorithm is analyzed. The result shows that the MDL tolerance of the proposed algorithm is similar with the constrained FD-LMS algorithm.

2. Principle

2.1 Description of the Unconstrained FD-LMS Algorithm

Fig. 1 shows the structure of the unconstrained adaptive FD-LMS algorithm for the output of mode i ($1 \leq i \leq M$). The received signal $u_j(n)$ ($1 \leq j \leq M$) is twofold-oversampled sequence. The serial data $u_j(n)$ is firstly converted into paralleled data $u_j^e(n)$ and $u_j^o(n)$ to enable half-symbol-spacing filter [26]. We suppose that the length of each block is N and we choose an overlap-and-save factor of 0.5 as a result of implementing easily. The FD input vector $\mathbf{U}_j^{e,o}(k)$ contains the current block and

the previous block, which can be written as

$$\mathbf{U}_j^{e,o}(k) = \text{diag}\{\mathbf{F}[u_j^{e,o}(kN - N), \ldots, u_j^{e,o}(kN + N - 1)]\} \tag{1}$$

Where diag{ · } is a diagonal matrix, and $\mathbf{F}$ is the 2N × 2N discrete Fourier transform (DFT) matrix. Then, we define the initial FD filter vector $\mathbf{W}_{i,j}^{e,o}(0)$ as

$$\mathbf{W}_{i,j}^{e,o}(0) = \mathbf{F}[\mathbf{w}_{i,j}^{e,o}(0), \mathbf{0_N}]^{\mathrm{T}} \tag{2}$$

Where the coefficient $\mathbf{w}_{i,j}^{e,o}(0) = [w_{i,j,0}^{e,o}(0), \ldots, w_{i,j,N}^{e,o}(0)]$. And $\mathbf{0_N}$ is an N dimensional row vector, elements of which are all zero. The FD vector $\mathbf{Y}_i(k)$ with column length of 2N is shown as

$$\mathbf{Y}_i(k) = \sum_{j=1}^{\mathrm{M}} \sum_{p=\mathrm{e,o}} \mathbf{U}_j^p(k) \cdot \mathbf{W}_{i,j}^p(k) \tag{3}$$

For the accuracy of the gradient estimation, TD error signal is multiplexed by a phase fluctuation $\exp(\mathrm{j}\phi(k))$ to avoid the impact of laser phase noise [10], which is the carrier phase estimation (CPE) module in Fig. 1. The error vector in TD is given as

$$\mathbf{e}_i(k) = (\mathbf{d}_i(k) - \mathbf{y}_i(k)) \cdot \exp(\mathrm{j}\phi(k)) \tag{4}$$

Where $\mathbf{d}_i(k)$ is the desired signal. As the overlap-and-save method is used, we take the latter block as the TD output $\mathbf{y}_i(k)$. Then, the corresponding FD error vector $\mathbf{E}_i(k)$ is given as

$$\mathbf{E}_i(k) = \mathbf{FGe}_i(k) = (\mathbf{FGd}_i(k) - \mathbf{FQF}^{-1}\mathbf{Y}_i(k)) \cdot \exp(\mathrm{j}\phi(k)) \tag{5}$$

Where $\mathbf{G} = [\,\mathbf{0_N}\ \mathbf{I_N}\,]$, and the 2N × 2N matrix $\mathbf{Q} = \mathbf{GG}^{\mathbf{T}} = \begin{bmatrix} \mathbf{0_N} & \mathbf{0_N} \\ \mathbf{0_N} & \mathbf{I_N} \end{bmatrix}$. Where $\mathbf{I_N}$ is an N × N identity matrix. The TD constraint process of the constrained FD-LMS algorithm is given as

$$\varphi_{ij}^{e,o}(k) = \text{The first N data of } \mathbf{F}^{-1}[\text{conj}\{\mathbf{U}_j^{e,o}(k)\} \otimes \mathbf{E}_i(k)] \tag{6}$$

$$\Phi_{ij}^{e,o}(k) = \mathbf{F}[\varphi_{ij}^{e,o}(k); \mathbf{O_N}] \tag{7}$$

The tap-updating equation for the constrained FD-LMS algorithm is given as

$$\mathbf{W}_{i,j}^{e,o}(k+1) = \mathbf{W}_{i,j}^{e,o}(k) + 2\mathbf{D}_{i,j}^{e,o}(k) \cdot \Phi_{ij}^{e,o}(k) \tag{8}$$

Where $\mathbf{D}_{i,j}^{e,o}(k) = \text{diag}\{\mu_{i,j,0}^{e,o}(k), \ldots, \mu_{i,j,\mathrm{M}-1}^{e,o}(k)\}$ is the step -size matrix and $[\cdot]^{\mathrm{H}}$ denotes Hermitian conjugate. Elements of the step-size matrix balance the convergence speed and MSE of the algorithm. The unconstrained FD-LMS algorithm saves the pair of FFT and IFFT in (6) and (7). The FD tap-updating equation for the unconstrained FD-LMS algorithm is given as

$$\mathbf{W}_{i,j}^{e,o}(k+1) = \mathbf{W}_{i,j}^{e,o}(k) + 2\mathbf{D}_{i,j}^{e,o}(k) \cdot [\mathbf{U}_j^{e,o}(k)]^{\mathrm{H}} \cdot \mathbf{E}_i(k) \tag{9}$$

2.2 Derivation of Step-Size for the Unconstrained FD-LMS Algorithm

In the unconstrained FD-LMS algorithm, all elements of $\mathbf{D}_{i,j}^{e,o}(k)$ are fixed. It limits the convergence speed of the algorithm. Then, we use the bin-wise block-varying step-size control method in [25] to obtain step-size of each frequency bin of each block. The method has been proven to be highly sensitive to noise disturbance [11].

We define posterior error to calculate step-size of each frequency bin in each block [25]. The TD posterior error vector $\mathbf{p}_i(k)$ with row length of N is given as

$$\mathbf{p}_i(k) = \mathbf{d}_i(k) - \mathbf{QF}^{-1} \sum_{j=1}^{\mathrm{M}} \sum_{p=\mathrm{e,o}} \mathbf{U}_j^p(k) \cdot \mathbf{W}_{i,j}^p(k+1) \tag{10}$$

As $\mathbf{FQF}^{-1} = 1/2\mathbf{I}_{2N}$ [27], and combining (5), (9) and (10). The FD posterior error vector $\mathbf{P}_i(k)$ is given as

$$\mathbf{P}_i(k) = \left\{ \mathbf{I}_{2N} - \sum_{j=1}^{M} \sum_{p=e,o} \mathbf{D}_{i,j}^{p}(k) \cdot \mathbf{U}_j^{p}(k) \cdot [\mathbf{U}_j^{p}(k)]^{H} \right\} \cdot \mathbf{E}_i(k) \tag{11}$$

The FD posterior error of the mth ($m = 1,\ldots, 2N$) frequency bin is

$$\mathrm{P}_{i,m}(k) = \left\{ 1 - \sum_{j=1}^{M} \sum_{p=e,o} \mu_{i,j,m}^{p} \cdot \mathrm{U}_{j,m}^{p}(k) \cdot [\mathrm{U}_{j,m}^{p}(k)]^{H} \right\} \cdot \mathrm{E}_{i,m}(k) \tag{12}$$

Taking the mean square of both sides of (12), we could have

$$\mathrm{S}_{p,i,m}(k) = \left(1 - \sum_{j=1}^{M} \sum_{p=e,o} \mu_{i,j,m}^{p}(k) \cdot \mathrm{S}_{u,j,m}^{p}(k) \right) \cdot \mathrm{S}_{e,i,m}(k) \tag{13}$$

Where

$$\mathrm{S}_{p,i,m} = \mathrm{E}[|\mathrm{P}_{i,m}(k)|^2] \tag{14}$$

$$\mathrm{S}_{u,j,m}^{e,o} = \mathrm{E}[|\mathrm{U}_{j,m}^{e,o}(k)|^2] \tag{15}$$

$$\mathrm{S}_{e,i,m} = \mathrm{E}[|\mathrm{E}_{i,m}(k)|^2] \tag{16}$$

Where E[·] denotes the statistical expectation. In MDM system with additive Gaussian white noise (AWGN) channel, we consider that the posterior error converges to the background noise after equalization. Therefore, we have

$$\mathrm{S}_{p,i,m} = \mathrm{S}_{v,i,m} \tag{17}$$

Where $\mathrm{S}_{v,i,m}$ is the power spectral density (PSD) of the background noise. We consider that all the equalizers converge at the same rate. Then, we could derive the step-size of each equalizer as

$$\mu_{i,j,m}^{e,o}(k) = \frac{\alpha}{\mathrm{S}_{u,j,m}^{e,o}(k)} \left(1 - \sqrt{\frac{\mathrm{S}_{v,i,m}(k)}{\mathrm{S}_{e,i,m}(k)}} \right) \tag{18}$$

Where α is the adaption rate. We can find that the step-size is controlled by $\mathrm{S}_{v,i,m}(k)$ from (18). Here, we use the method of magnitude squared coherent (MSC) function in [28] to estimate $\mathrm{S}_{v,i,m}(k)$. We obtain

$$\mathrm{S}_{v,i,m}(k) = \mathrm{S}_{e,i,m}(k) \left(1 - \frac{\left| \mathrm{S}_{ex,i,j,m}^{e,o}(k) \right|^2}{\mathrm{S}_{e,i,m}(k) \cdot \mathrm{S}_{u,j,m}^{e,o}(k)} \right) \tag{19}$$

Where $\mathrm{S}_{ex,i,j,m}^{e,o}(k)$ is the cross power spectral density (PSD) between $\mathbf{e}_i(k)$ and $\mathrm{u}_j^{e,o}(n)$. Then, the final values of $\mu_{i,j,m}^{e,o}(k)$ can be written as

$$\mu_{i,j,m}^{e,o}(k) = \frac{\alpha}{\mathrm{S}_{u,j,m}^{e,o}(k)} \left(1 - \sqrt{1 - \frac{\left| \mathrm{S}_{ex,i,j,m}^{e,o}(k) \right|^2}{\mathrm{S}_{e,i,m}(k) \cdot \mathrm{S}_{u,j,m}^{e,o}(k)}} \right) \tag{20}$$

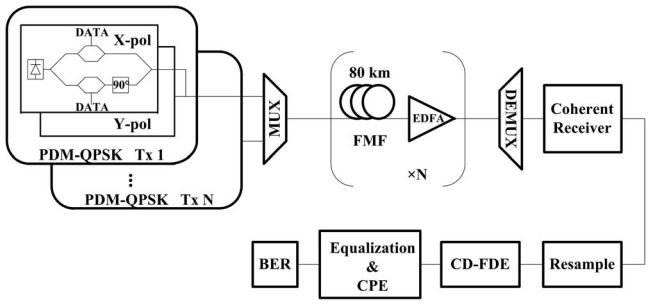

Fig. 2. Block diagram of the simulated system.

Since the input signal $u_j^{e,o}(n)$ and error signal $\mathbf{e}_i(k)$ are known, the recursively smoothing method is used to estimate these related PSDs, which are given as

$$S_{u,j,m}^{e,o}(k) = \lambda S_{u,j,m}^{e,o}(k-1) + (1-\lambda)\left|\mathbf{U}_j^{e,o}(k)\right|^2 \tag{21}$$

$$S_{e,i,m}(k) = \lambda S_{e,i,m}(k-1) + (1-\lambda)\left|\mathbf{E}_i(k)\right|^2 \tag{22}$$

$$S_{ex,i,j,m}^{e,o}(k) = \lambda S_{ex,i,j,m}^{e,o}(k-1) + (1-\lambda)[\mathbf{U}_j^{e,o}(k)]^{\mathrm{H}} \cdot \mathbf{E}_i(k) \tag{23}$$

Where λ $(0 < \lambda < 1)$ is the forgetting factor.

2.3 Complexity Analysis

In an M $\times$ M MDM system, total complexity of the equalization algorithm can be measured by the number of complex multiplications per symbol per mode. For the conventional FD-LMS algorithm, to obtain one symbol each mode, we need 4M multiplications between input block and equalizers as shown in (3). As for the updating equation in (9), it needs 4M multiplications between error block and conjugate transpose of input block. To achieve noise-directing, we need additional complex multiplications. The recursion equations of (21)–(23) require 2, 2 and 4M complex multiplications per symbol per mode respectively. We consider that division and square root have the same hardware complexity [29], so the algorithm needs another 8M complex multiplications for (20).

As a result of omitting the TD constraint of (6) and (7), the unconstrained FD-LMS algorithm only requires 4 FFTs per mode per symbol [18]. We suppose that the radix-2 FFT is used, then 4 FFTs take up $4\log_2 2N$ complex multiplications per symbol per mode.

Therefore, for each output per symbol, the complexity of the constrained FD-LMS algorithm is given as

$$C_1 = (4M + 4)\log_2 2N + 8M \tag{24}$$

The complexity of the unconstrained FD-LMS algorithm is shown as

$$C_2 = 4\log_2 2N + 8M \tag{25}$$

And the complexity of the proposed algorithm is given as

$$C_3 = 4\log_2 2N + 20M + 4 \tag{26}$$

3. Simulation

3.1 System Model

To verify the effectiveness of the proposed variable step-size unconstrained FD-LMS algorithm, three representative MIMO-MDM systems are investigated in this work, which are respectively over 2-LP-mode MIMO FMF [17], 2-LP-mode weakly-coupled FMF [30], 4-LP-mode MIMO FMF [31]. The simulation setup is shown in Fig. 2. At the transmitter, lasers with line-width of 100 kHz operate

TABLE 1
Characteristics of the FMFs

Type	Attenuation (dB/km)	CD [ps/(nm·km)]				DMGD (ps/km)			
		LP_{01}	LP_{11}	LP_{21}	LP_{02}	LP_{01}	LP_{11}	LP_{21}	LP_{02}
2-LP-mode MIMO FMF	0.2	20	21	–	–	0	27	–	–
2-LP-mode weakly-coupled FMF	0.2	21	26	–	–	0	4400	–	–
4-LP-mode MIMO FMF	0.2	21	26	19	8	0	27	54	54

at 1550 nm and $2^{23} - 1$ sequence is modulated onto each mode in the format of quadrature phase shift keying (QPSK) with bit rates of 56 Gb/s. The modulated signals are then combined by mode-multiplexer (MUX) and coupled into FMF. Detailed parameters of three kinds of FMFs are shown in Table 1. The model of the few mode fibers (FMF) are similar to the one in [32]. The FMFs are composed of many spans. To simulate random mode coupling, each span is divided into sections. All modes are considered to propagate independently in each section. Therefore, the delay is added to mode LP_{11} (LP_{02} and LP_{21}) at the end of each section, and the mode coupling happens at the end of each section. In this paper, the length of each section is 10 km [17]. For the 2-LP-mode MIMO FMF and the 4-LP-mode MIMO FMF, we set the coupling factor to -30 dB/km. For the 2-LP-mode weakly-coupled FMF, the coupling factors are -38 dB/km and -30 dB/km for LP_{01}/LP_{11} and LP_{11a}/LP_{11b} respectively. The few mode erbium-doped fiber amplifier (FM-EDFA) is added at the end of every 80 km to compensate the span loss. Variable noise is added after FMF to set different values of OSNR (0.1nm optical noise reference bandwidth). At the receiver, mode-demultiplexer (DEMUX) is used to separate these modes, which are then fed into the coherent receivers.

In the offline digital signal process (DSP), the received signals are firstly resampled to 2 samples per symbol, and then chromatic dispersion (CD) compensation module is used to compensate the CD of the FMF. The conventional constrained FD-LMS algorithm in [10], the unconstrained FD-LMS algorithm in [22] and the variable step-size unconstrained FD-LMS algorithm are applied in the equalization module independently. To pursue better performance, two stages of CPE are used in our simulation. One is inside the phase of initial channel estimation and the other lies in the phase of decision-directed estimation to further alleviate laser phase noise [10]. Finally, bit error ratio (BER) is calculated.

3.2 Simulation Results

In our simulation, the first 10% symbols were used as the training sequence. The tap length of the filter is 2N, which is the same as the length of impulse response of the FMF [10]. Firstly, the equalization performance is simulated in three systems with three different kinds of fibers. Then the convergence speed and the influence of MDL is explored over the 2-LP-mode MIMO FMF.

The system with 2-LP-mode MIMO FMF needs a 6×6 MIMO DSP and the 4-LP-mode MIMO FMF needs a 12×12 MIMO DSP [33]. However, the system over 2-LP-mode weakly-coupled FMF needs a 2×2 MIMO DSP for the LP_{01} mode group and a 4×4 MIMO DSP for the LP_{11} mode group [34]. Figs. 3 and 4 show the BER performance as a function of OSNR for the proposed algorithm on six modes over 2-LP-mode weakly-coupled FMF and 4-LP-mode MIMO FMF respectively. It can be seen that the proposed algorithm perform well in these systems. Fig. 3 shows that a small variability of the BER for LP_{01} mode group and the LP_{11} mode group, it is less than 0.5 dB at the

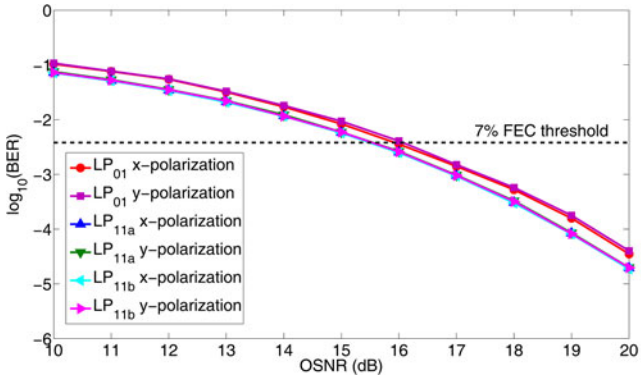

Fig. 3. BER performance versus OSNR on six modes over 2-LP-mode weakly coupled FMF for variable step-size unconstrained FD-LMS algorithm.

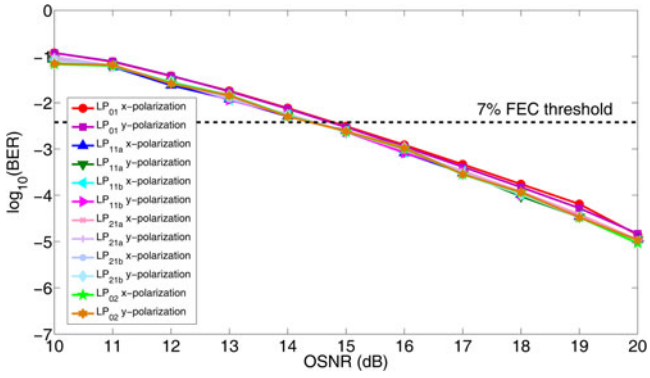

Fig. 4. BER performance versus OSNR on six modes over 2-LP-mode weakly coupled fiber for variable step-size unconstrained FD-LMS algorithm.

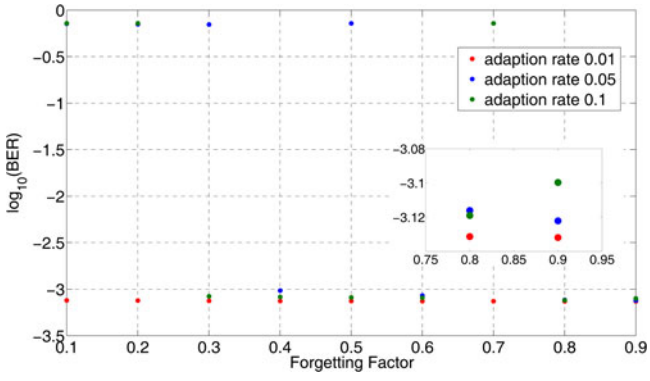

Fig. 5. Optimal forgetting factor for the variable step-size unconstrained FD-LMS algorithm.

7% FEC threshold. In Fig. 4, the least needed OSNR of all 12 tributes at the 7% FEC threshold is about 14.3 dB, and the other tributes need a OSNR penalty within 0.3 dB.

In order to neglect the influence of the forgetting factor on the proposed algorithm, the optimal value is first acquired as shown in Fig. 5. The transmission distance is 80 km and the OSNR is 15 dB. The accumulated DMGD is 2.16 ns, so we set the FFT size to be 128 to it. The optimal value of the forgetting factor is based on the x-polarization of LP_{01} mode, and other modes have similar results. When the adaption rate is 0.01, we can take any value from 0 to 1 as the forgetting factor.

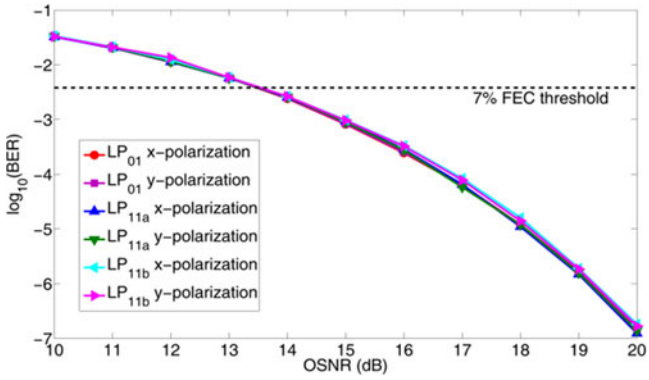

Fig. 6. BER performance versus OSNR on six modes for variable step-size unconstrained FD-LMS algorithm.

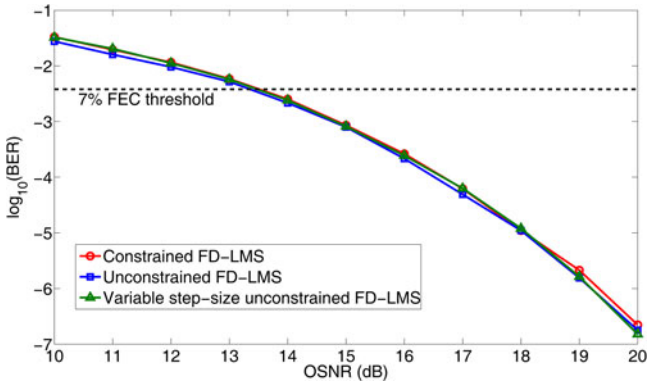

Fig. 7. BER performance comparison of three algorithms: BER versus OSNR.

However, as adaption rate increases, the span of λ decreases. The reason is that higher adaption rate can induce higher error, thus narrowing range of the forgetting factor. As is shown in the figure, the value of 0.8 shows the best BER performance over the other values of forgetting factor in all conditions. Therefore, λ is set to 0.8 in our simulation.

To fully evaluate the equalization performance of the variable step-size unconstrained FD-LMS algorithm, we set different OSNR values and different link distances for our simulation. The transmission distances in Figs. 6 and 7 are both 80 km. Fig. 6 shows the BER performance as a function of OSNR for the proposed algorithm on six modes over 6-mode MIMO FMF. As OSNR increases, BER of six modes decrease at almost the same rate. At the 7% FEC threshold, OSNR for all six modes are about 13.5 dB. The BER comparison of three equalization algorithms for x-polarization of mode LP_{01} at different OSNR levels is plotted in Fig. 7. It can be seen that all three algorithms perform well in demultiplexing and show similar BER performance.

Fig. 8 compares the BER performance of three algorithms as the link distances sweep from 0 to 2000 km. We neglect the effect of the MDL here. The OSNR is set to 22 dB and the values are the average of all six channels. For fair comparison, we employ the same sub-filter length and the same initial matrix for each algorithm at the same link distance. As the distance increases, the total DMGD accumulates and the required size of FFT enlarges [10]. At a distance of 2000 km, the total DMGD increases to 54 ns and the FFT size is set to 2048. From the figure, we can see that the BER performances of three algorithms are almost the same for transmission distance shorter than 600 km. When the distance is higher than 1000 km, the proposed algorithm is slightly worse than the constrained FD-LMS algorithm, but it is still superior to the unconstrained FD-LMS algorithm. At a distance of 2000 km, the BER of the proposed algorithm close to the 7% FEC threshold.

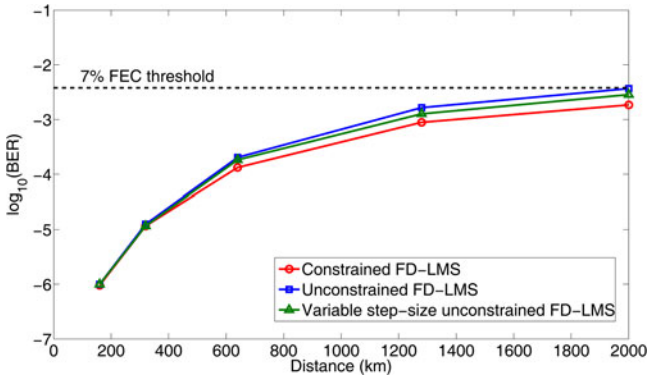

Fig. 8. BER performance comparison of three algorithms BER versus distance.

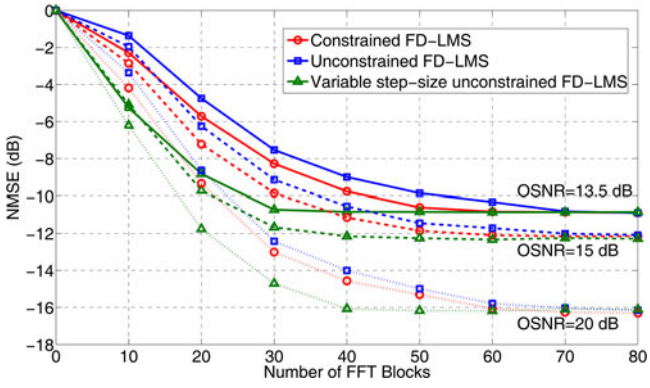

Fig. 9. Convergence speed comparison of three algorithms at different OSNR levels.

In FD block-adaptive equalization, convergence speed of an algorithm can be measured by the least required number of FFT blocks to converge. Fig. 9 shows the convergence speed comparison of three algorithms at different OSNR levels. The distance is 80 km and the FFT size is 128. According to Fig. 9, when the OSNR is 13.5 dB, the constrained FD-LMS algorithm and the unconstrained FD-LMS algorithm require 51 and 65 FFT blocks to reach the same normalized MSE (NMSE) of -10.8 dB respectively, while the variable step-size unconstrained FD-LMS algorithm only needs 28 FFT blocks. Thus, the proposed variable step-size unconstrained algorithm improves the convergence speed by 45.1% and 56.9% compared with constrained FD-LMS algorithm and unconstrained FD-LMS algorithm respectively. It also can be seen that as OSNR increases, convergence speed enhancement decreases slightly. It is obvious that the variable step-size method improves the convergence speed of the unconstrained FD-LMS greatly. Fig. 10 shows the comparison on needed number of symbols to converge to -12 dB NMSE at different distances for three algorithms. It can be seen that a longer distance needs more symbols for convergence, and the convergence speed improvement of the proposed algorithm is further enhanced in systems with longer distance.

Based on the complexity analysis in 2.3, the complexity comparison of three algorithms in terms of distance is shown in Fig. 11. It can be seen that as the distance increases, the complexity of the proposed variable step-size method increases slowly as the unconstrained FD-LMS algorithm does, which is much different from the constrained FD-LMS algorithm. Table 2 shows the detailed data comparison of the constrained FD-LMS algorithm and the proposed algorithm in Fig. 8. At a transmission distance of 2000 km, the FFT size is 2048 and the proposed algorithm reduces the complexity by 52.8% compared to the constrained FD-LMS algorithm. Fig. 12 shows the number of complex multiplications for all three algorithms is in relation to number of modes. The size of FFT is 128. As a result of adding variable step-size method, the complexity of the proposed equalization

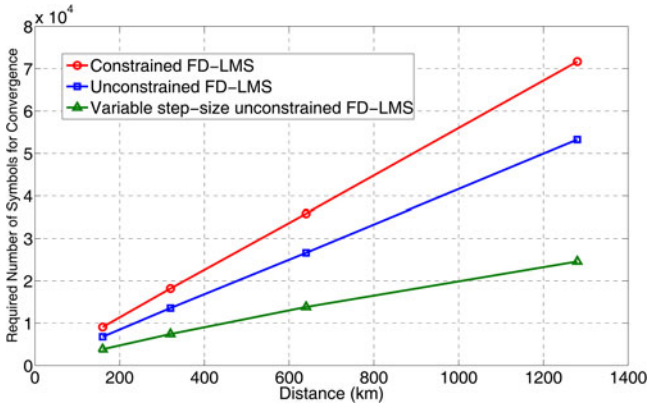

Fig. 10. Convergence speed comparison of three algorithms at different distances.

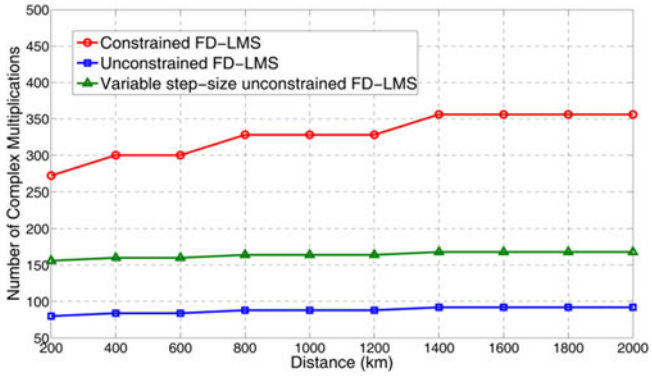

Fig. 11. Complexity comparison of three algorithms: number of complex multiplications versus distance.

TABLE 2
Complexity Comparison of the Constrained FD-LMS Algorithm and the Proposed Algorithm

Distance	Constrained FD-LMS	Variable step-size unconstrained FD-LMS
1000 km	328	164
2000 km	356	168

algorithm is higher than the unconstrained FD-LMS algorithm. However, the result shows that the complexity of the variable step-size unconstrained FD-LMS algorithm is still significantly lower than the constrained FD-LMS algorithm.

Finally, we explored the effect of MDL on our proposed algorithm. The MDL is modeled by introducing an amplifier gain difference between LP01 group modes and LP11 group modes [31], which is set to 0.5 dB in our simulation. After every 80 km, MDL is added. The mode coupling keeps unchanged. Fig. 13 shows the performance comparison of the constrained FD-LMS algorithm, unconstrained FD-LMS the proposed algorithm in terms of OSNR penalty with algorithm and respect to no-MDL configuration for a BER the proposed algorithm in terms of OSNR penalty with algorithm and respect to no-MDL configuration for a BER target of 10^{-3}. The transmission distance

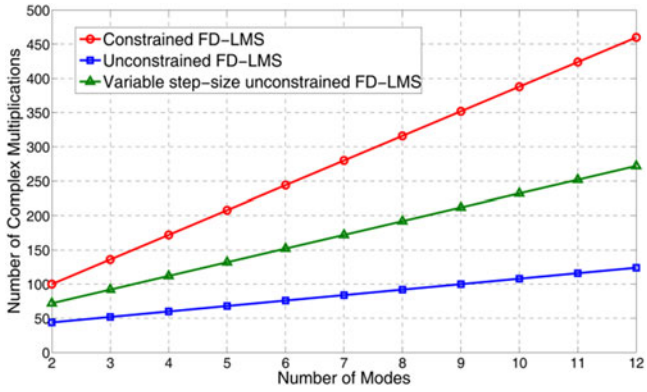

Fig. 12. Complexity comparison of three algorithms: number of complex multiplications versus number of modes.

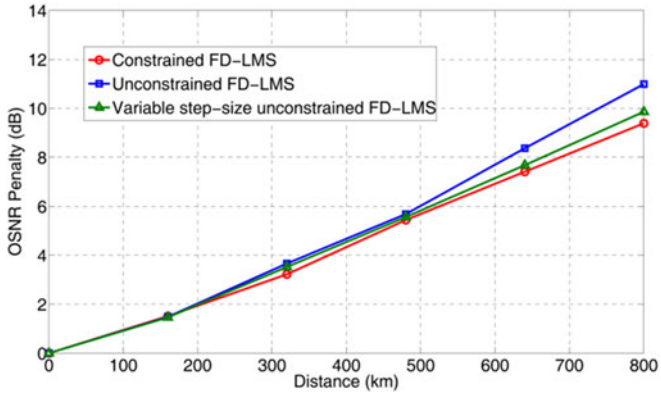

Fig. 13. OSNR Penalty versus distance for three algorithms.

is from 0 to 800 km. It can be seen that longer distance induces more OSNR penalty for three algorithms. The OSNR penalty of the proposed algorithm is 0.5 dB higher than the constrained FD-LMS algorithm.

4. Conclusion

In this paper, a variable step-size unconstrained FD-LMS algorithm is proposed for demultiplexing the signals on different modes in MDM transmission. The proposed variable step-size unconstrained adaptive FD-LMS algorithm shows similar BER performance with the unconstrained FD-LMS algorithm and the constrained FD-LMS algorithm. However, it improves the convergence speed by 45.1% and 56.9% with respect to the constrained FD-LMS algorithm and the unconstrained FD-LMS algorithm. For a six-mode transmission of 2000 km, compared with the constrained FD-LMS algorithm, the complexity of the proposed algorithm reduces 52.8%. In addition, the proposed algorithm shows similar MDL tolerance with the constrained FD-LMS algorithm.

References

[1] G. Li, N. Bai, N. Zhao, and C. Xia, "Space-division multiplexing: The next frontier in optical communication," *Adv. Opt. Photon.*, vol. 6, no. 4, pp. 5041–5046, Dec. 2014.

[2] D. J. Richardson, J. M. Fini, and L. E. Nelson, "Space-division multiplexing in optical fibres," *Nature Photon.*, vol. 7, no. 5, pp. 354–362, Apr. 2013.

[3] P. J. Winzer and G. J. Foschini, "MIMO capacities and outage probabilities in spatially multiplexed optical transport systems," *Opt. Exp.*, vol. 19, no. 17, pp. 16680–11696, Aug. 2011.

[4] N. Bai *et al.*, "Mode-division multiplexed transmission with inline few-mode fiber amplifier," *Opt. Exp.*, vol. 20, no. 3, pp. 2668–2680, Jan. 2012.

[5] S. O. Arik, K. P. Ho, and J. Kahn, "Group delay management and multi-input multi-output signal processing in mode-division multiplexing systems," *J. Lightw. Technol.*, vol. 34, no. 11, pp. 2867–2880, Jun. 2016.

[6] K. P. Ho and J. M. Kahn, "Mode coupling and its impact on spatially multiplexed systems," in *Optical Fiber Telecommunications VI*. Amsterdam, The Netherlands: Elsevier, 2013.

[7] Y. Li, N. Hua, X. Zheng, and G. Li, "Impact of mode coupling on the capacity of mode-division multiplexing networks with MIMO equalization," in *Proc. 2016 Opt. Fiber Commun. Conf. Exhib.*, Anaheim, CA, USA, 2016, Paper Tu2H.5.

[8] R. Ryf *et al.*, "Space-division multiplexing over 10 km of three-mode fiber using coherent 6 $\times$ 6 MIMO processing," in *Proc. 2011 Nat. Fiber Opt. Eng. Conf. Opt. Fiber Commun. Conf. Expo.*, Los Angeles, CA, USA, Mar. 2011, Paper PDPB10.

[9] S. O. Arik, D. Askarov, and J. M. Kahn, "Adaptive frequency-domain equalization in mode-division multiplexing systems," *J. Lightw. Technol.*, vol. 32, no. 32, pp. 1841–1852, May 2014.

[10] N. Bai and G. Li, "adaptive frequency-domain equalization for mode-division multiplexed transmission," *IEEE Photon. Technol. Lett.*, vol. 24, no. 21, pp. 1918–1921, Nov. 2012.

[11] X. He, Y. Weng, and Z. Pan, "A step-size controlled method for fast convergent adaptive FD-LMS algorithm in few-mode fiber communication systems," *J. Lightw. Technol.*, vol. 32, no. 22, pp. 4422–4428, Nov. 2014.

[12] Z. Yang, J. Zhao, N. Bai, and G. Li, "A feasible adaptive recursive least square frequency-domain algorithm for equalization of mode-division multiplexed fiber transmission," in *Proc. Asia Commun. Phonon. Conf.*, Hong Kong, Nov. 2015, Paper ASu5D.3.

[13] X. He, X. Zhou, J. Wang, Y. Weng, and Z. Pan, "A fast convergence frequency domain least mean square algorithm for compensation of differential mode group delay in few mode fibers," in *Proc. 2013 Opt. Fiber Commun. Conf. Expo. Nat. Fiber Opt. Eng. Conf.*, Anaheim, CA, USA, Mar. 2013, Paper OM2C.4.

[14] Y. Weng, T. Wang, and Z. Pan, "Fast-convergent adaptive frequency-domain recursive least-squares algorithm with reduced complexity for MDM transmission systems using optical few-mode fibers," in *Proc. 2016 Conf. Lasers Electro-Opt.*, San Jose, CA, USA, Jun. 2016, pp. 1–2.

[15] Z. Yang, J. Zhao, N. Bai, E. Ip, T. Wang, and G. Li, "Experimental demonstration of adaptive recursive least square frequency-domain equalization for long-distance mode-division multiplexed transmission," in *Proc. Eur. Conf. Opt. Commun.*, Sept. 2015, pp. 1–3.

[16] B. Inan *et al.*, "DSP complexity of mode-division multiplexed receivers," *Opt. Exp.*, vol. 20, no. 10, pp. 10859–10869, 2012.

[17] L. Yan and G. Hu, "A fast and efficient frequency-domain-independent component analysis for MDM transmission," *IEEE Photon. Technol. Lett.*, vol. 28, no. 26, pp. 1778–1781, Aug. 2016.

[18] S. S. Hayking, *Adaptive Filter Theory*, 4th ed. Englewood Cliffs, NJ, USA: Prentice-Hall, 2001.

[19] M. S. Faruk, "Unconstraint adaptive frequency-domain equalizer for coherent optical receivers," in *Proc. 8th Int. Conf. Electr. Comput. Eng.*, Dec. 2014, Paper Th2A.39.

[20] J. J. Shynk, "Frequency-domain and multirate adaptive filtering," *IEEE Signal Process. Mag.*, vol. 9, no. 1, pp. 14–37, Jan. 1992.

[21] M. S. Faruk, "Unconstraint adaptive frequency-domain equalizer for coherent optical receivers," in *Proc. 8th Int. Conf. Electr. Comput. Eng.*, Dhaka, Bangladesh, Dec. 2014, pp. 40–42.

[22] S. Randel, P. J. Winzer, M. Montoliu, and R. Ryf, "Complexity analysis of adaptive frequency-domain equalization for MIMO-SDM transmission," in *Proc. Eur. Conf. Exhib. Opt. Commun.*, 2013, pp. 1–3.

[23] J. C. Lee and K. U. Chong, "Performance analysis of frequency-domain block LMS adaptive digital filters," *IEEE Trans. Circuits Syst.*, vol. 36, no. 2, pp. 173–189, Feb. 1989.

[24] T. Aboulnasr and K. Mayyas, "A robust variable step-size LMS-type algorithm: Analysis and simulations," *IEEE Trans. Signal Process.*, vol. 45, no. 3, pp. 631–639, Mar. 1997.

[25] K. Shi and X. Ma, "A frequency domain step-size control method for LMS algorithms," *IEEE Signal Process. Lett.*, vol. 17, no. 2, pp. 125–128, Feb. 2010.

[26] M. S. Faruk and K. Kikuchi, "Adaptive frequency-domain equalization in digital coherent optical receivers," *Opt. Exp.*, vol. 19, no. 13, pp. 12789–12798, Jun. 2011.

[27] Y. Huang and J. Benssty, *Audio Signal Processing for Next Generation Multimedia Communication Systems*. Norwell, MA, USA: Kluwer, 2004.

[28] K. Shi, X. Ma, and G. T. Zhou, "A residual echo suppression technique for systems with nonlinear acoustic echo paths," in *Proc. IEEE Int. Conf. Acoust., Speech Signal Process.*, 2008, pp. 257–260.

[29] E. M. Schwarz and M. J. Flynn, "Using a floating-point multiplier's internals for high-radix division and square root," Stanford Univ., Stanford, CA, USA, Tech. Rep. CSL-TR-93-554, 1993.

[30] P. Sillard, M. Bigot-Astruc, and D. Boivin, "Few-mode fiber for uncoupled mode-division multiplexing transmissions," in *Proc. Eur. Conf. Expo. Opt. Commun.*, Geneva, Switzerland, 2011, Paper Tu.5.LeCervin.7.

[31] Y. Tian, J. Li, and P. Zhu, "Quantification of MDL-induced signal degradation in MIMO-OFDM mode-division multiplexing systems," *Opt. Exp.*, vol. 24, no. 17, pp. 18948–18959, Aug. 2016.

[32] J. Vuong, P. Ramantanis, and A. Seck, "Understanding discrete linear mode coupling in few-mode fiber transmission systems," in *Proc. Eur. Conf. Exhib. Opt. Commun.*, Geneva, Switzerland, 2011, Paper Tu.5.B.2.

[33] P. Sillard, "Few-mode fibers for space division multiplexing," in *Proc. 2016 Opt. Fiber Commun. Conf. Exhib.*, Los Angeles, CA, USA, 2016, Paper Th1J.1.

[34] P. Genevaux, M. Salsi, and A. Boutin, "Comparison of QPSK and 8-QAM in a three spatial modes transmission," *IEEE Photon. Technol. Lett.*, vol. 26, no. 4, pp. 414–417, Feb. 2014.